On the cross-sectional measurement points necessary for point correlation dimension analysis of two-phase flow

Akio Suzuki[†] and Masaki Misawa[†]

†National Institute of Advanced Industrial Science and Technology (AIST)
1-2 Namiki, Tsukuba, Ibaraki, 305-8564 Japan
Email: akio.suzuki@aist.go.jp

Abstract– This study experimentally investigated cross-sectional measuring points necessary for point correlation dimension analysis of fully developed slug flow. Applying an optimal delay time reconstruction method and a point correlation dimension method to cross-sectional void fraction time series greatly improves the reliability of analyses. Results show that nine-point averaging is sufficient for a broad range of airflow rates. When the air flow rate is low, one-point measurement, except in the area near a pipe wall, yields reliable results.

1. Introduction

Studies of low-dimensional chaos provide new analytical methods: nonlinear time series analyses [1]. The methods are powerful tools for understanding irregular time series generated by a low-dimensional nonlinear system. Nonlinear time series analyses are applied increasingly to complex time series from the real world, including those of human electroencephalographic (EEG) data, financial data, and two-phase flow data [2–3]. However, the estimation of invariants is difficult and sometimes becomes subjective; the reliability of estimated results has not been shown sufficiently. We examined nonlinear time series analyses of two-phase flow time series to improve the reliability of analytical methods and to support useful applications such as validation of numerical simulation results and early detection of irregular states. Two-phase flow offers some advantages over EEG or financial data: flow complexity is controllable and stationary long-term data are obtainable.

For two reasons, estimation becomes difficult: analytical methods and measurement methods. The correlation dimension of two-phase flow is typically greater than four. However, all analysis results we know were estimated using methods that was originally proposed in the 1980s for a low-dimensional chaotic system. Differential pressure sensors are widely used to obtain flow data. However, pressure fluctuations throughout a flow system are transmitted to the sensor with a delay: they act as noise. Therefore, direct measurement of the local flow state is appropriate.

We showed that applying an optimal delay time reconstruction method [4] and a point correlation dimension method [5] to cross-sectional averaging void fraction time series greatly improves the reliability of

analysis in terms of passing a surrogate data test [6]. The next step is the estimation of error and the proposition of analysis and measurement methods to reduce the error.

This paper describes an experimental investigation of the effect of coarse-resolution void fraction measurement. In early analyses, we used 184-point cross-sectional void fraction distributions measured using a 16×16 wire-mesh sensor [7]. A longer measurement with a higher sampling rate is possible if the number of wires can be reduced without spoiling the reliability or increasing the error. The flow disturbance caused by the wires also becomes small. First, the void fraction time series that were calculated using 3×3, 2×2 and 1×3 wires were analyzed and compared to those of 16×16 wires. Next, the time series that were made using only 1×1 wires were analyzed. Analytical results and their surrogate data test results are shown.

2. Estimation of point correlation dimension

Nonlinear time series analyses are based on the reconstruction of an orbit in phase space from the time series. The most common reconstruction technique is the use of delays. State vectors $z(k)$ in an m-dimensional phase space are formed from time-delayed values of the scalar time series $x(k)$:

$$z(k) = [x(k), x(k+\tau), \cdots, x(k+(m-1)\tau)]^T, \quad (1)$$

where m and τ are respectively called an embedding dimension and a delay.

In almost all analyses of two-phase flow, the delay τ is determined by the relation between $x(k)$ and $x(k+\tau)$: their autocorrelation and mutual information. A salient problem is that optimization between $x(k)$ and $x(k+\tau)$ does not imply the optimization of other elements such as $x(k+2\tau)$, ..., $x(k+(m-1)\tau)$. The problem becomes more serious for larger embedding dimensions m. Many methods have been proposed to estimate the optimal delay time τ (reviewed in [8]). We used artificially generated quasiperiodic time series to evaluate some of them, and chose the average displacement method [4], which gives the most robust results.

The average displacement method measures the average distance $S(\tau)$ of the reconstructed vector $z(k)$ in Eq. (1) from the m dimensional space's main diagonal.

$$S(\tau) = \frac{1}{N} \sum_{i=1}^{N} \sqrt{\sum_{j=1}^{m-1} (x(i+j\cdot\tau) - x(i))^2} \qquad (2)$$

The main drawback of this method is that no theoretical reason exists for the τ-determining rule. We examined some criteria and found that a better result is obtained at the first minimum of the slope of $S(\tau)$.

The point correlation dimension is a locally defined fractal dimension at a specific point in an orbit. This method was proposed by Skinner *et al.* [5] for analyses of physiological time series such as those of EEGs. The procedure resembles that of Grassberger and Procaccia (GP) method, except that it calculates a local correlation sum $C_i(r)$ at a reference point $z(i)$.

$$C_i(r) = \frac{1}{N_{pair}} \sum_{\substack{j=1 \\ |i-j|>w}}^{N} \Theta(r - |z(i) - z(j)|) \qquad (3)$$

$$C_i(r) \propto r^{PD_2(i)}, \text{ for } r \to 0 \text{ and } N \to \infty \qquad (4)$$

The scaling exponent of $C_i(r)$ represents the local point correlation dimension $PD_2(i)$ at each reference point. Averaging $PD_2(i)$ over all reference points yields the (averaged) point correlation dimension PD_2, which gives a global description of the geometrical structure of an orbit. Determination of a scaling region is required for each reference point to obtain PD_2. We use an automatic procedure based on a local slope approach [5].

3. Experiments and analysis results
3.1 Flow loop and measurement system

A schematic of the experimental flow loop is shown in Fig. 1. Gas that is provided by an air compressor is controlled by a regulator; a pump controls water flow. A 2.1-m-long acrylic pipe with 42 mm inner diameter is used as a vertical test section. A mixing chamber is located at the vertical pipe's inlet, where air through a distributed nozzle plate (nozzle diameter is 5 mm) and water are mixed. The nozzle diameter is sufficiently large to allow air bubbles to unite and form a series of large bubbles. This flow state is called slug flow. In vertical flow, the bubbles are an axially symmetrical bullet shape that occupies almost the entire cross-sectional area of the pipe. After passing through the vertical pipe, air is released to the atmosphere, whereas water is circulated.

The vertical pipe is equipped with a wire-mesh sensor. HM Prasser (FZR, Germany) developed the wire-mesh sensor to provide real-time tomographic view of cross-sectional void fraction (volumetric air-water rate) distribution [7]. Two layers of thin parallel wires are extended across the cross section with a vertical distance of 1.6 mm (Fig. 2). A pulse is sent sequentially along the sender wires, on which an electric field is formed instantaneously at each node. When a bubble enters a node, the electric field is deformed and the electrical conductivity between the sender wire and the receiver wire are reduced proportional to the local void fraction.
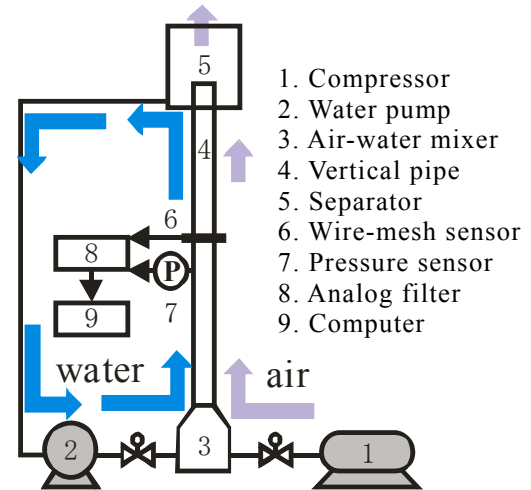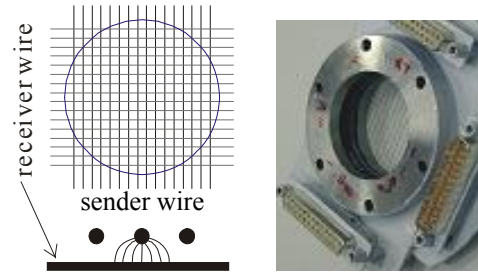

Fig. 1 Schematic of two-phase flow system

1. Compressor
2. Water pump
3. Air-water mixer
4. Vertical pipe
5. Separator
6. Wire-mesh sensor
7. Pressure sensor
8. Analog filter
9. Computer

Fig. 2 Wire-mesh sensor

t=0.45   t=0.5   t=0.55

(a) Instantaneous 184-point cross-section distribution (superficial velocity of gas Jg=1.2 m/s)

(b) Axial distribution (8th receiver wire, Jg=1.2 m/s)

(c) Axial distribution (8th receiver wire, Jg=3.6 m/s)

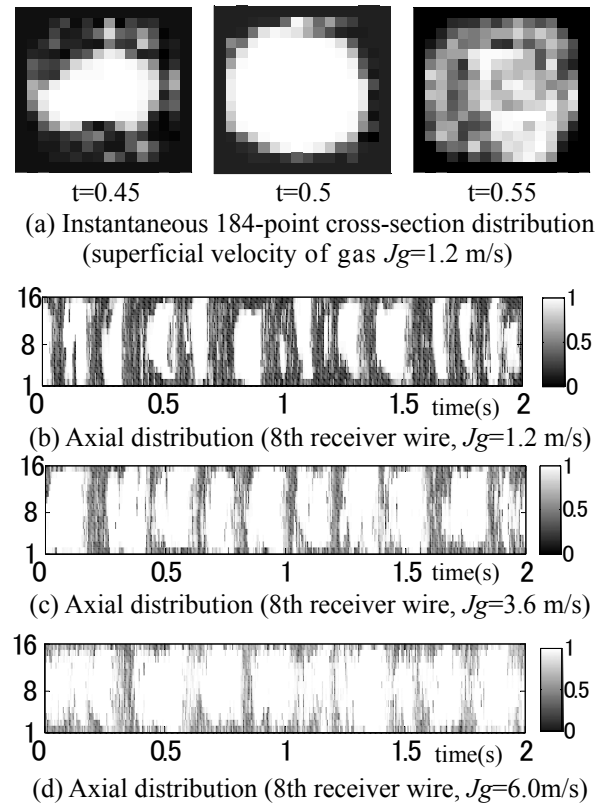(d) Axial distribution (8th receiver wire, Jg=6.0m/s)

Fig. 3 Void fraction distribution of slug flow

The wire-mesh sensor is located at about 1.1 m from the vertical pipe inlet (length-to-diameter ratio L/D=25.7).

A 16 × 16 wire-mesh sensor is used for the 42-mm-diameter pipe. The measuring point pitch is 2.63 mm and the effective measuring points number is 184. Examples of measured wire-mesh sensor data are shown in Fig. 3.

3.2 Conditions of experiments and analyses

All two-phase flow experiments were carried out on the natural circulation condition (the water pump was off). Void fraction distributions were measured for eight flow conditions (volumetric flow rates Qg=10, 30, 50, 100, 200, 300, 400, 500 l/min; corresponding to superficial velocity Jg=Qg/(cross-sectional area of a pipe)=0.12, 0.36, 0.60, 1.20, 2.41, 3.61, 4.81, 6.02 m^3/s). Void fractions were recorded for 30 s through an anti-alias analog low-pass filter at a sampling rate of 1000 Hz (cut-off frequency is 200 Hz). A FIR digital low-pass filter was applied to the time series to remove sensor noise (cut-off frequency is 98 Hz).

In all analyses, the number of reference points Nr, which were chosen randomly, were set to 5% of the size of the time series (Nr=1500).

The reliability of the estimated results was tested using a surrogate data method. We chose the null hypothesis of the test that the original time series is generated from a linear stochastic process possibly undergoing a nonlinear static transform. We then shuffled the original time series randomly and created 39 surrogate data sets, which had the identical spectrum and distribution as the original time series (significance level α=0.05), using the free nonlinear time series analysis package TISEAN [1].

3.3 Effect of spatially coarse measurement

The necessary spatial resolution of void fraction measurement is investigated. The combinations of selected sender and receiver wires are as follows.

9-point (3 × 3): [sender, receiver]=[(4, 8, 12), (4, 8, 12)]
4-point (2 × 2): [sender, receiver]=[(4, 12), (4, 12)]
3-point (1 × 3): [sender, receiver]=[(8), (4, 8, 12)]

Cross-sectional void fraction time series were calculated by averaging the measurement of points. Examples of time series are shown in Fig. 4. The point correlation dimensions PD_2 on various flow conditions are shown in Fig. 5. All PD_2 pass the surrogate data tests. The PD_2 of the 184-point averaged time series increases and tends to converge to a constant value when the superficial velocity Jg is increased: the PD_2 curves of 9-points and 184-points are similar. The PD_2 curve of the 4-point time series is much higher than that of the 184-point time series. The increases are explainable as follows. For the four-point measurement, all measurement points are located near a wall area. The local void fraction near the wall position is sensitive to deformation of bubbles. This newly apparent movement increases the PD_2.

The PD_2 curve of three-point time series differs greatly in the high airflow rate domain: PD_2 are much lower and do not converge because of the saturation of the void
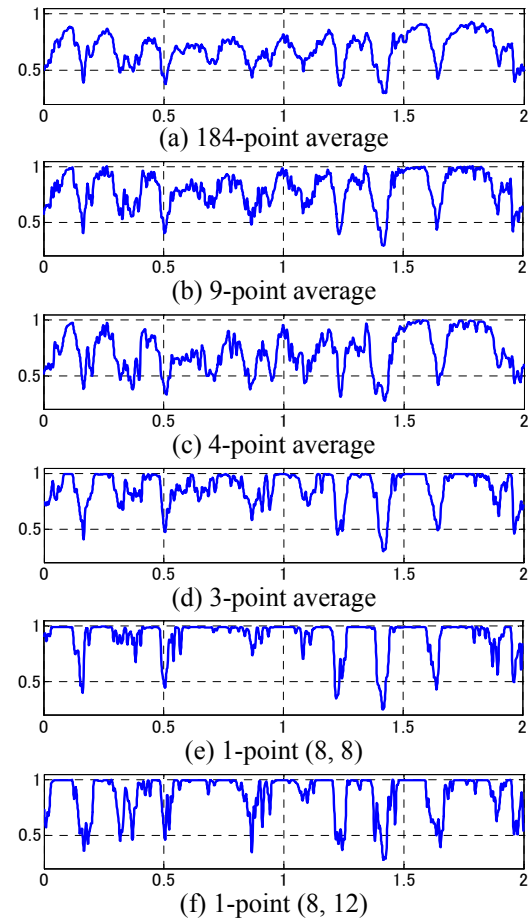

(a) 184-point average

(b) 9-point average

(c) 4-point average

(d) 3-point average

(e) 1-point (8, 8)

(f) 1-point (8, 12)

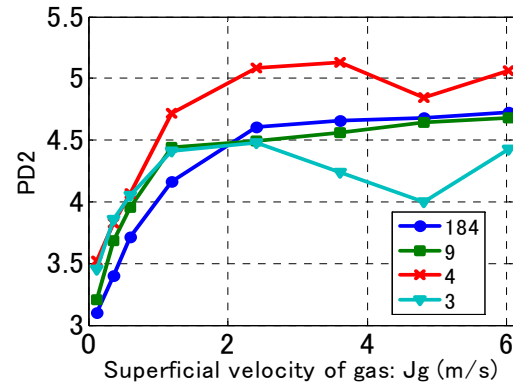Fig. 4 Example of void fraction time series (Jg=4.8 m/s)

Fig. 5 PD_2 of 184-, 9-, 4-, and 3-point averaging void fraction time series

fraction (Fig. 4d). The spatial resolution is too coarse. For that reason, measurement is easily saturated and the information on a bubble motion is lost.

These results show that the measurement of nine points in the cross-section (3 × 3 wires) is needed to estimate the point correlation dimension. Large error arises if the spatial resolution becomes lower. However, it is noteworthy that this conclusion is true only for fully developed slug flow, in which large bullet-shaped bubbles span most of the pipe cross-section. Finer spatial

resolution is necessary when bubbles are allowed to move to a transverse direction.

3.4 One-point void fraction time series

We investigated the possibility of estimating the point correlation dimension from a one-point void fraction. We selected the 8th sender wire and analyzed 14 one-point void fraction time series. Examples are shown in Fig. 4e and 4f. Results are listed in Table 1. Except for the two nearest to the pipe wall, all PD_2 pass the surrogate data tests. Two-phase flow in a vertical pipe is axial symmetric. Therefore, identical results are obtained at other places in a cross-section.

The PD_2 distribution of slug flow (Jg=1.2 m/s) is shown in Fig. 6. The PD_2 tends to become low as a measurement point goes to the central part.

The PD_2 of a one-point void fraction versus Jg are shown in Table 2. All estimation results pass the surrogate data test when the airflow rate is low ($Jg \leq$1.2 m/s), but tests tended to fail in the high airflow rate range ($Jg \geq$2.4 m/s). We infer that those unreliable results are caused by the overly long saturated time of the void fraction.

4. Conclusion

We have experimentally investigated cross-sectional void fraction measuring points that are necessary for point-correlation dimension analysis of fully developed slug flow. Analyses of various flow conditions show that spatially very coarse resolution is sufficient only if it passes a surrogate data test. However, to estimate the nearly identical dimensional values to those of spatially fine resolution time series in broad airflow range, a symmetrical nine-point measurement is needed. One-point measuring void fraction time series were also analyzed. Except for the time series measured near a pipe wall, statistically reliable results are obtained only in a low airflow rate range. The obtained results include large error, but the cross-sectional distribution of point correlation dimension is obtainable.

Acknowledgments

References

[1] H. Kantz and T. Schreiber, "Nonlinear Time Series Analysis", Cambridge University Press, 1997.

[2] C. M. Van den Bleek, M. O. Coppens, and J. C. Schouten, "Application of chaos analysis to multiphase reactors", Chem. Eng. Sci., Vol.57, pp.4763-4778, 2002.

[3] F. Johnsson, et al., "Characterization of fluidization regimes by time-series analysis of pressure fluctuations", Int. J. of Multiphase Flow, Vol.26, pp.663-715, 2000.

[4] M. T. Rosenstein, et al., "Reconstruction expansion as a geometry-based framework for choosing proper delay times", Physica D, Vol.73, pp.82-98, 1994.

[5] J. E. Skinner, et al., "The point correlation dimension: performance with nonstationary surrogate data and noise",

Table.1 PD_2 and surrogate data test results of one-point void fraction time series (Jg=1.2 m/s)

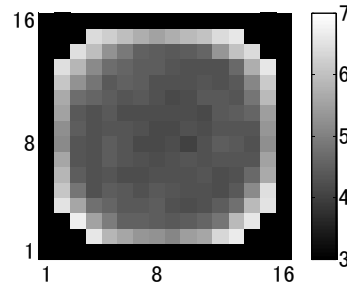| Receiver wire No.	PD2	Test	Receiver wire No.	PD2	test
2	5.37	Fail	9	4.25	pass
3	4.37	Pass	10	4.20	pass
4	4.35	Pass	11	4.44	pass
5	4.39	Pass	12	4.39	pass
6	4.35	Pass	13	4.42	pass
7	4.14	Pass	14	4.20	pass
8	4.19	Pass	15	5.40	fail

sender wire No. 8

Fig. 6 Cross sectional PD2 distribution of one-point void fraction time series (Jg=1.2 m/s)

Table 2 PD_2 of one-point void fraction time series

Receiver wire No.	Jg	PD2	Test	Receiver wire No.	Jg	PD2	test
8	0.12	3.69	Pass	12	0.12	3.83	pass
8	0.36	3.76	Pass	12	0.36	4.04	pass
8	0.60	4.22	Pass	12	0.60	4.14	pass
8	1.20	4.20	Pass	12	1.20	4.50	pass
8	2.41	3.88	Fail	12	2.41	4.50	fail
8	3.61	3.49	Pass	12	3.61	4.05	fail
8	4.81	3.59	Fail	12	4.81	3.75	pass
8	6.02	3.73	Fail	12	6.02	4.11	fail

sender wire No. 8

Integrative Physiological and Behavioral Science, Vol.29, pp.217-234, 1994.

[6] A. Suzuki and M. Misawa, "Reliable correlation dimension estimation method for analyzing two-phase flow", Proceedings of NOLTA 2004, 2004.

[7] H. M. Prasser, et al., "A new electrode-mesh tomograph for gas-liquid flows", Flow Measurement and Instrumentation, Vol. 9, pp.111-119, 1998.

[8] A. Galka, "Topics in Nonlinear Time Series Analysis", World Scientific Publishing, 2000.